

MATHEMATICAL MODELLING AND ANALYSIS  
Volume 22 Number 3, May 2017, 373–388  
<https://doi.org/10.3846/13926292.2017.1313329>  
© Vilnius Gediminas Technical University, 2017

Publisher: Taylor&Francis and VGTU  
<http://www.tandfonline.com/TMMA>  
ISSN: 1392-6292  
eISSN: 1648-3510

# Numerical Study of Rosenau-KdV Equation Using Finite Element Method Based on Collocation Approach

Turgut Ak<sup>a</sup>, Sharanjeet Dhawan<sup>b</sup>,  
S. Battal Gazi Karakoc<sup>c</sup>, Samir K. Bhowmik<sup>d</sup> and  
Kamal R. Raslan<sup>e</sup>

<sup>a</sup>*Department of Transportation Engineering, Yalova University*  
77100 Yalova, Turkey

<sup>b</sup>*Department of Mathematics, Central University of Haryana*  
123029 Haryana, India

<sup>c</sup>*Department of Mathematics, Nevsehir Haci Bektas Veli University*  
50300 Nevsehir, Turkey

<sup>d</sup>*Department of Mathematics, University of Dhaka*  
1000 Dhaka, Bangladesh

<sup>e</sup>*Department of Mathematics, Al-Azhar University*  
Nasr-City, Cairo, Egypt  
E-mail(*corresp.*): [akturgut@yahoo.com](mailto:akturgut@yahoo.com)

Received December 1, 2016; revised March 25, 2017; published online May 15, 2017

**Abstract.** In the present paper, a numerical method is proposed for the numerical solution of Rosenau-KdV equation with appropriate initial and boundary conditions by using collocation method with septic B-spline functions on the uniform mesh points. The method is shown to be unconditionally stable using von-Neumann technique. To check accuracy of the error norms  $L_2$  and  $L_\infty$  are computed. Interaction of two and three solitary waves are used to discuss the effect of the behavior of the solitary waves during the interaction. Furthermore, evolution of solitons is illustrated by undular bore initial condition. These results show that the technique introduced here is suitable to investigate behaviors of shallow water waves.

**Keywords:** Rosenau-KdV, B-spline, finite element, collocation and dispersive.

**AMS Subject Classification:** 35Q53; 76B15; 76M10; 65L60; 41A15.

## 1 Introduction

In engineering and real world scene, a wave is a disturbance that travels through space and time. Different types of waves occur in nature having different kind of applications. Dynamics of shallow water waves that are observed along

lake shores and beaches have been an active research area for the past few decades [1, 2, 8, 9, 22]. Specifically, the Korteweg-de Vries (KdV) equation

$$U_t + aUU_x + bU_{xxx} = 0$$

is a generic model for the study of nonlinear shallow water waves [10]. But, it has a number of shortcomings as it describes a unidirectional propagation of waves; thus wave-wave, wave-wall interactions cannot be treated by the KdV equation. Secondly, because it was derived under the assumption of weak anharmonicity, both the shape and the behavior of high-amplitude waves cannot be predicted well by the KdV. Keeping in view these shortcomings, the Rosenau equation

$$U_t + \lambda U_x + cU_{xxxxt} + d(U^2)_x = 0$$

was derived [17]. In addition to Rosenau equation, for the consideration of the nonlinear wave, we further add the viscous term  $U_{xxx}$ . The resulting equation is then called Rosenau-KdV equation

$$U_t + aU_x + bU_{xxx} + cU_{xxxxt} + d(U^2)_x = 0. \quad (1.1)$$

A detailed information about the existence of Rosenau-KdV equation can be collected from [16, 17, 25]. Study of these models has reported quite interesting results, which are available in literature [3, 12, 14, 15, 19].

Recently, many researchers have used different schemes such as homotopy perturbation method, reductive perturbation technique, tanh method and sine-cosine method, the tanh-coth method, first integral method [5] to study the solution profile of Rosenau-KdV equation. The generalized Rosenau-KdV equation is studied by using the sech-ansatz method [6]. Further, the topological 1-soliton solution of the generalized Rosenau-KdV equation is obtained [18]. Some finite difference schemes for the solution of Rosenau-KdV equation and the generalized Rosenau-KdV equation can be seen in [7, 24]. The conservation laws of the Rosenau-KdV-RLW equation are computed with power law nonlinearity by the aid of multiplier approach in Lie symmetry analysis [13, 23]. A numerical approach with a new formulation for a nonlinear wave proposed by coupling the Rosenau-KdV equation and the Rosenau-RLW equation is presented.

This work is dedicated to the numerical simulations of the Rosenau-KdV equation so that it can be analyzed in detail. The content of this paper is organized as follows. In the next section, we consider the governing Rosenau-KdV equation and introduce septic B-spline basis functions. Section 3 describes the solvability of collocation finite element method in detail. In Section 4 and 5, stability of the proposed method with convergence rate is discussed. The results on validation of proposed method of solution are presented in Section 6 which includes study of motion of single solitary wave, interaction of two solitary waves, interaction of three solitary waves and evolution of solitons. We make a detailed comparison with available data in order to confirm and illustrate our theoretical analysis. Finally, we finish our paper by concluding remarks in the last section.

## 2 The governing equation and septic B-Spline basis functions

In this section, Rosenau-KdV equation will be considered with the physical boundary conditions  $U \rightarrow 0$  and  $x \rightarrow \pm\infty$ , where  $a, b, c$  and  $d$  are arbitrary parameters and the subscripts  $x$  and  $t$  denote the spatial and temporal differentiations, respectively.

In order to be able to apply the numerical method, solution region of the problem is restrained over an interval  $a \leq x \leq b$ . Space interval  $[a, b]$  is separated into uniformly sized finite elements of length  $h$  by the knots  $x_m$  like that  $a = x_0 < x_1 < \dots < x_N = b$ . Lengths of these finite elements are  $h = (b - a)/N = (x_{m+1} - x_m)$  for  $m = 1, 2, \dots, N$ .

The equation (1.1) will be solved by choosing

$$\begin{aligned}
 U(a, t) = 0, \quad U(b, t) = 0, \quad U_x(a, t) = 0, \\
 U_x(b, t) = 0, \quad U_{xx}(a, t) = 0, \quad U_{xx}(b, t) = 0, \quad t > 0
 \end{aligned}$$

homogeneous boundary conditions and

$$U(x, 0) = f(x) \quad , \quad a \leq x \leq b,$$

the initial condition.

The septic B-spline approximation functions  $\phi_m(x)$  are defined as

$$\phi_m(x) = \frac{1}{h^7} \begin{cases} (x - x_{m-4})^7, & [x_{m-4}, x_{m-3}], \\ (x - x_{m-4})^7 - 8(x - x_{m-3})^7, & [x_{m-3}, x_{m-2}], \\ (x - x_{m-4})^7 - 8(x - x_{m-3})^7 + 28(x - x_{m-2})^7, & [x_{m-2}, x_{m-1}], \\ (x - x_{m-4})^7 - 8(x - x_{m-3})^7 + 28(x - x_{m-2})^7 \\ \quad - 56(x - x_{m-1})^7, & [x_{m-1}, x_m], \\ (x_{m+4} - x)^7 - 8(x_{m+3} - x)^7 + 28(x_{m+2} - x)^7 \\ \quad - 56(x_{m+1} - x)^7, & [x_m, x_{m+1}], \\ (x_{m+4} - x)^7 - 8(x_{m+3} - x)^7 + 28(x_{m+2} - x)^7, & [x_{m+1}, x_{m+2}], \\ (x_{m+4} - x)^7 - 8(x_{m+3} - x)^7, & [x_{m+2}, x_{m+3}], \\ (x_{m+4} - x)^7, & [x_{m+3}, x_{m+4}], \\ 0, & elsewhere, \end{cases} \tag{2.1}$$

at the knots  $x_m$  over the interval  $[a, b]$  for  $m = -3(1)N + 3$  [11]. All spline functions apart from  $\phi_{m-3}(x), \phi_{m-2}(x), \phi_{m-1}(x), \phi_m(x), \phi_{m+1}(x), \phi_{m+2}(x), \phi_{m+3}(x)$  are zero over the element  $[x_m, x_{m+1}]$ . Each septic B-spline covers eight elements so that each element  $[x_m, x_{m+1}]$  is covered by eight splines [11]. The values of  $\phi_m(x)$  and its derivatives may be tabulated as in Table 1.

**Table 1.** Septic B-spline function and its derivatives at nodes  $x_m$ .

$x$	$x_{m-4}$	$x_{m-3}$	$x_{m-2}$	$x_{m-1}$	$x_m$	$x_{m+1}$	$x_{m+2}$	$x_{m+3}$	$x_{m+4}$
$\phi_m$	0	1	120	1191	2416	1191	120	1	0
$h\phi'_m$	0	-7	-392	-1715	0	1715	392	7	0
$h^2\phi''_m$	0	42	1008	630	-3360	630	1008	42	0
$h^3\phi'''_m$	0	-210	-1680	3990	0	-3990	1680	210	0
$h^4\phi^{iv}_m$	0	840	0	-7560	13440	-7560	0	840	0
$h^5\phi^{iv}_m$	0	-2520	10080	-12600	0	12600	-10080	2520	0
$h^6\phi^{vi}_m$	0	5040	-30240	75600	-100800	75600	-30240	5040	0

The set of these approximation functions  $\{\phi_{-3}(x), \phi_{-2}(x), \phi_{-1}(x), \dots, \phi_{N+1}(x), \phi_{N+2}(x), \phi_{N+3}(x)\}$  forms a basis for approximate solution which will be defined over  $[a, b]$ . A global approximation  $U_N(x, t)$  is stated in terms of the septic B-spline approximation functions as

$$U_N(x, t) = \sum_{i=-3}^{N+3} \phi_i(x)\delta_i(t), \tag{2.2}$$

where  $\delta_i(t)$  are time dependent parameters determined from the boundary and collocation conditions.

Substituting trial function (2.1) into equation (2.2), the nodal values of  $U, U', U'', U''', U^{iv}, U^v$  and  $U^{vi}$  are obtained in terms of the element parameters  $\delta_m$  by

$$\begin{aligned}
 U_m &= \delta_{m-3} + 120\delta_{m-2} + 1191\delta_{m-1} + 2416\delta_m + 1191\delta_{m+1} + 120\delta_{m+2} + \delta_{m+3}, \\
 U'_m &= \frac{7}{h}(-\delta_{m-3} - 56\delta_{m-2} - 245\delta_{m-1} + 245\delta_{m+1} + 56\delta_{m+2} + \delta_{m+3}), \\
 U''_m &= \frac{42}{h^2}(\delta_{m-3} + 24\delta_{m-2} + 15\delta_{m-1} - 80\delta_m + 15\delta_{m+1} + 24\delta_{m+2} + \delta_{m+3}), \\
 U'''_m &= \frac{210}{h^3}(-\delta_{m-3} - 8\delta_{m-2} + 19\delta_{m-1} - 19\delta_{m+1} + 8\delta_{m+2} + \delta_{m+3}), \\
 U^{iv}_m &= \frac{840}{h^4}(\delta_{m-3} - 9\delta_{m-1} + 16\delta_m - 9\delta_{m+1} + \delta_{m+3}), \\
 U^v_m &= \frac{2520}{h^5}(-\delta_{m-3} + 4\delta_{m-2} - 5\delta_{m-1} + 5\delta_{m+1} - 4\delta_{m+2} + \delta_{m+3}), \\
 U^{vi}_m &= \frac{5040}{h^6}(\delta_{m-3} - 6\delta_{m-2} + 15\delta_{m-1} - 20\delta_m + 15\delta_{m+1} - 6\delta_{m+2} + \delta_{m+3}).
 \end{aligned} \tag{2.3}$$

### 3 Collocation finite element method

Now, we identify the collocation points with the knots and using equation (2.3) to evaluate  $U_m$ , its necessary space derivatives and substitute into equa-

tion (1.1) to obtain the set of the coupled ordinary differential equations

$$\begin{aligned} &\dot{\delta}_{m-3} + 120\dot{\delta}_{m-2} + 1191\dot{\delta}_{m-1} + 2416\dot{\delta}_m + 1191\dot{\delta}_{m+1} + 120\dot{\delta}_{m+2} + \dot{\delta}_{m+3} \\ &+ \frac{7a}{h}(-\delta_{m-3} - 56\delta_{m-2} - 245\delta_{m-1} + 245\delta_{m+1} + 56\delta_{m+2} + \delta_{m+3}) \\ &+ \frac{210b}{h^3}(-\delta_{m-3} - 8\delta_{m-2} + 19\delta_{m-1} - 19\delta_{m+1} + 8\delta_{m+2} + \delta_{m+3}) \\ &+ \frac{840c}{h^4}(\dot{\delta}_{m-3} - 9\dot{\delta}_{m-1} + 16\dot{\delta}_m - 9\dot{\delta}_{m+1} + \dot{\delta}_{m+3}) \\ &+ \frac{7dZ_m}{h}(-\delta_{m-3} - 56\delta_{m-2} - 245\delta_{m-1} + 245\delta_{m+1} + 56\delta_{m+2} + \delta_{m+3}) = 0, \end{aligned} \tag{3.1}$$

where  $\cdot$  denotes derivative with respect to time. For the linearization technique, we assume that the quantity  $U$  in the non-linear term  $UU_x$  in equation (1.1) is locally constant. In this case, the term  $U$  is taken as

$$Z_m = \delta_{m-3} + 120\delta_{m-2} + 1191\delta_{m-1} + 2416\delta_m + 1191\delta_{m+1} + 120\delta_{m+2} + \delta_{m+3}.$$

If time parameters  $\delta_i$ 's and its time derivatives  $\dot{\delta}_i$ 's in equation (3.1) are discretized by the Crank-Nicolson formula and usual finite difference approximation, respectively,

$$\delta_i = \frac{\delta_i^{n+1} + \delta_i^n}{2}, \quad \dot{\delta}_i = \frac{\delta_i^{n+1} - \delta_i^n}{\Delta t},$$

a recurrence relationship between two time levels  $n$  and  $n + 1$  is obtained in terms of two unknown parameters  $\delta_i^{n+1}$ ,  $\delta_i^n$  for  $i = m - 3, m - 2, \dots, m + 2, m + 3$ :

$$\begin{aligned} &\gamma_1\delta_{m-3}^{n+1} + \gamma_2\delta_{m-2}^{n+1} + \gamma_3\delta_{m-1}^{n+1} + \gamma_4\delta_m^{n+1} + \gamma_5\delta_{m+1}^{n+1} + \gamma_6\delta_{m+2}^{n+1} + \gamma_7\delta_{m+3}^{n+1} \\ &= \gamma_7\delta_{m-3}^n + \gamma_6\delta_{m-2}^n + \gamma_5\delta_{m-1}^n + \gamma_4\delta_m^n + \gamma_3\delta_{m+1}^n + \gamma_2\delta_{m+2}^n + \gamma_1\delta_{m+3}^n, \end{aligned} \tag{3.2}$$

where

$$\begin{aligned} \gamma_1 &= [1 - E(a + dZ_m) - M + K], \\ \gamma_2 &= [120 - 56E(a + dZ_m) - 8M], \\ \gamma_3 &= [1191 - 245E(a + dZ_m) + 19M - 9K], \\ \gamma_4 &= [2416 + 16K], \\ \gamma_5 &= [1191 + 245E(a + dZ_m) - 19M - 9K], \\ \gamma_6 &= [120 + 56E(a + dZ_m) + 8M], \\ \gamma_7 &= [1 + E(a + dZ_m) + M + K], \\ m &= 0, 1, \dots, N, \quad E = \frac{7}{2h}\Delta t, \quad M = \frac{105b}{h^3}\Delta t, \quad K = \frac{840c}{h^4}\Delta t. \end{aligned}$$

The system (3.2) consists of  $(N + 1)$  linear equations including  $(N + 7)$  unknown parameters  $(\delta_{-3}, \delta_{-2}, \delta_{-1}, \dots, \delta_{N+1}, \delta_{N+2}, \delta_{N+3})^T$ . To obtain a unique solution for this system, we need six additional constraints. These are obtained

from the boundary conditions and can be used to eliminate  $\delta_{-3}, \delta_{-2}, \delta_{-1}$  and  $\delta_{N+1}, \delta_{N+2}, \delta_{N+3}$  from the system (3.2) which then becomes a matrix equation for the  $N + 1$  unknowns  $d = (\delta_0, \delta_1, \dots, \delta_N)^T$  of the form

$$Ad^{n+1} = Bd^n.$$

The matrices  $A$  and  $B$  are septa-diagonal  $(N + 1) \times (N + 1)$  matrices and this matrix equation can be easily solved. Two or three inner iterations are applied to the term  $\delta^{n*} = \delta^n + \frac{1}{2}(\delta^n - \delta^{n-1})$  at each time step to cope with the non-linearity caused by  $Z_m$ . Before the commencement of the solution process, initial parameters  $d^0$  must be determined by using the initial condition and the following derivatives at the boundaries:

$$\begin{aligned} U_N(x, 0) &= U(x_m, 0), \quad m = 0, 1, 2, \dots, N, \\ (U_N)_x(a, 0) &= 0, \quad (U_N)_x(b, 0) = 0, \\ (U_N)_{xx}(a, 0) &= 0, \quad (U_N)_{xx}(b, 0) = 0, \\ (U_N)_{xxx}(a, 0) &= 0, \quad (U_N)_{xxx}(b, 0) = 0. \end{aligned}$$

So we have the following matrix form for the initial vector  $d^0$  :

$$Wd^0 = C,$$

where  $W$  is the matrix,  $d^0 = (\delta_0, \delta_1, \delta_2, \dots, \delta_{N-2}, \delta_{N-1}, \delta_N)^T$  and

$$C = [U(x_0, 0), U(x_1, 0), \dots, U(x_{N-1}, 0), U(x_N, 0)]^T.$$

### 4 Stability analysis

The stability analysis is based on the von Neumann theory. The growth factor  $\xi$  of the error in a typical mode of amplitude

$$\delta_m^n = \xi^n e^{imkh}, \tag{4.1}$$

where  $k$  is the mode number and  $h$  the element size, is determined from a linearization of the numerical scheme. Substituting the Fourier mode (4.1) into (3.2) gives the following equality

$$\begin{aligned} &\gamma_1 \xi^{n+1} e^{i(m-3)kh} + \gamma_2 \xi^{n+1} e^{i(m-2)kh} + \gamma_3 \xi^{n+1} e^{i(m-1)kh} + \gamma_4 \xi^{n+1} e^{imkh} \\ &\quad + \gamma_5 \xi^{n+1} e^{i(m+1)kh} + \gamma_6 \xi^{n+1} e^{i(m+2)kh} + \gamma_7 \xi^{n+1} e^{i(m+3)kh} \\ &= \gamma_7 \xi^n e^{i(m-3)kh} + \gamma_6 \xi^n e^{i(m-2)kh} + \gamma_5 \xi^n e^{i(m-1)kh} + \gamma_4 \xi^n e^{imkh} \\ &\quad + \gamma_3 \xi^n e^{i(m+1)kh} + \gamma_2 \xi^n e^{i(m+2)kh} + \gamma_1 \xi^n e^{i(m+3)kh}. \end{aligned} \tag{4.2}$$

Now, if Euler’s formula  $e^{ikh} = \cos(kh) + i \sin(kh)$  is used in equation (4.2) and this equation is simplified, we get the following growth factor:

$$\xi = (\omega - i\bar{\omega})/(\omega + i\bar{\omega}),$$

in which

$$\begin{aligned} \omega &= (2416+16\mu)+(2382-18\mu) \cos(kh)+240 \cos(2kh)+2(1+\mu) \cos(3kh), \\ \bar{\omega} &= 2(\beta - \lambda) \sin(kh) + (112\beta + 16\lambda) \sin(2kh) + (490\beta - 38\lambda) \sin(3kh), \end{aligned}$$

where

$$\beta = E(a + dZ_m), \quad \lambda = M, \quad \mu = K, \quad m = 0, 1, \dots, N - 1.$$

The modulus of  $|\xi|$  is 1, therefore the linearized scheme is unconditionally stable.

### 5 Error analysis

Splines and polynomials play a very important role in numerical approximations and mathematical analysis [20, 21]. A detailed analysis about the polynomial approximation and least squares piecewise polynomials approximations can be found in [4, 20, 21]. In this work, we use a higher order (septic) B-spline collocation scheme for the spatial approximation of the Rosenau-KdV equation. Now the main importance of using collocation scheme is that it gives super-convergence pointwise. Compared to the Galerkin inner product approach, the collocation approach does not require an extra integral to evaluate. So this approach is simpler and efficient to compute solutions.

Let  $H^r(\Omega)$  be the space of  $r$  times differentiable functions and  $\|\cdot\|_r$  be the standard  $H^r(\Omega)$  norm. Let  $v_h$  be an approximation to a function  $v(x) \in H^r(\Omega)$  in  $\Omega$ . Let  $h$  be the distance between the grids and  $\Omega = \cup_i \Omega_i$ , where  $\Omega_i = [x_i, x_{i+1}]$ ,  $x_{i+1} = x_i + h$ . We observe [20, 21] that

$$\|v(x) - v_h(x)\| \leq C\Delta x^{k+1} \|v\|_{k+1}, \quad 1 \leq k < r$$

and  $v_h$  stands for interpolation by piecewise-polynomials of degree  $r$  (considering  $\Omega = \cup_i \Omega_i$ ). This error is preserved by the Galerkin finite element approximation as well [21]. It can be easily observed [4] that if  $w_h$  is a suitable B splines defined by a polynomial of degree less or equal  $k$  then

$$\|w(x) - w_h(x)\| \leq C\Delta x^{l+1} \|w\|_{l+1}, \quad 1 \leq l < k$$

for any  $w \in H_k(\Omega)$ . In our study we use septic B-splines for space integration. The above discussion suggest a  $\mathcal{O}(\Delta x^8)$  accuracy for the spatial approximation in  $L_2(\Omega)$  norm. Since for time we use the Crank-Nicolson scheme which is of  $\mathcal{O}(\Delta t^2)$  accurate in  $L_2([0 T])$  norm for some  $T > 0$ ; followed by a forward difference scheme which is accurate of  $\mathcal{O}(\Delta t)$  accurate in  $L_2([0 T])$  norm for some  $T > 0$  [21]. So we obtain the error bound as

$$\|u(x, t) - u_h(x, t)\| \leq C_1\Delta x^8 + C_2\Delta t^2 + C_3\Delta t = C_1\Delta x^8 + C_2\Delta t, \quad (5.1)$$

for a suitable  $C_1 \geq 0$  and  $C_2 \geq 0$ .

## 6 Numerical simulations

Numerical results of the Rosenau-KdV equation are obtained for four test problems: the motion of single solitary wave, interaction of two and three solitary waves, evolution of solitons with undular bore initial condition. We use the error norm  $L_2$

$$L_2 = \|U^{exact} - U_N\|_2 \simeq \sqrt{h \sum_{j=1}^N |U_j^{exact} - (U_N)_j|^2}$$

and the error norm  $L_\infty$

$$L_\infty = \|U^{exact} - U_N\|_\infty \simeq \max_j |U_j^{exact} - (U_N)_j|, \quad j = 1, 2, \dots, N - 1$$

to calculate the difference between analytical and numerical solutions at some specified times. The two conserved quantities that equation (1.1) possess are given by

$$I_M = \int_a^b U dx \simeq h \sum_{j=1}^N U_j^n,$$

$$I_E = \int_a^b [U^2 + c(U_{xx})^2] dx \simeq h \sum_{j=1}^N [(U_j^n)^2 + c(U_{xx})_j^n],$$

which represent the momentum and energy of the shallow water waves, respectively [6]. In the simulation of solitary wave motion, the conserved quantities  $I_M$  and  $I_E$  are monitored to check the accuracy of the applied numerical method.

### 6.1 The motion of single solitary wave

The single solitary wave solution of the Rosenau-KdV equation (1.1) is given by being considered with the boundary conditions  $U \rightarrow 0$  as  $x \rightarrow \pm\infty$

$$U(x, t) = A \operatorname{sech}^4 [B(x - vt)],$$

in which

$$A = \frac{210bB^2}{13d}, \quad B = \frac{1}{3} \left[ \frac{-13ac + \sqrt{169a^2c^2 + 144b^2c}}{32bc} \right]^{\frac{1}{2}}, \quad v = \frac{b}{52cB^2}.$$

Also,  $a, b, c$  and  $d$  are arbitrary constants. The initial condition is taken as

$$U(x, 0) = A \operatorname{sech}^4 (Bx).$$

Firstly, the motion of the single solitary wave is modelled with parameters  $a = b = c = 1, d = 0.5$  and  $v = 1.18$  over the interval  $[-70, 100]$  for different values of space step ( $h$ ) and time step ( $\Delta t$ ). When the computations are done



**Table 2.** Comparison of conserved quantities for single solitary wave with  $a = b = c = 1$ ,  $d = 0.5$ ,  $v = 1.18$  and different values of  $h$  and  $\Delta t$ .

$h = \Delta t = 0.1$						
$t$	$I_M$			$I_E$		
	Present	CLDS [7]	SFEM [2]	Present	CLDS [7]	SFEM [2]
0	5.4981750556	5.4977225480	5.4981750556	1.9897841615	1.9845533653	1.9897841614
10	5.4981750556	5.4977249365	5.4981749939	1.9897841624	1.9845950759	1.9897841614
20	5.4981750556	5.4977287449	5.4981749598	1.9897841629	1.9846459641	1.9897841614
30	5.4981750555	5.4977319638	5.4981749423	1.9897841633	1.9846798272	1.9897841614
40	5.4981750621	5.4977342352	5.4981749335	1.9897841635	1.9847015013	1.9897841614
$h = \Delta t = 0.05$						
$t$	$I_M$			$I_E$		
	Present	CLDS [7]	SFEM [2]	Present	CLDS [7]	SFEM [2]
0	5.4981692134	5.4980606845	5.4981692134	1.9897831853	1.9843901753	1.9897831853
10	5.4981692136	5.4980608372	5.4981691962	1.9897831855	1.9844010295	1.9897831854
20	5.4981692136	5.4980610805	5.4981691829	1.9897831855	1.9844143675	1.9897831852
30	5.4981692134	5.4980612870	5.4981691736	1.9897831854	1.9844232703	1.9897831856
40	5.4981692116	5.4980613985	5.4981691629	1.9897831852	1.9844289740	1.9897831853
$h = \Delta t = 0.025$						
$t$	$I_M$			$I_E$		
	Present	CLDS [7]	SFEM [2]	Present	CLDS [7]	SFEM [2]
0	5.4981698357	5.4981454184	5.4981698357	1.9897809062	1.9849493353	1.9897809061
10	5.4981698365	5.4981454791	5.4981697751	1.9897809077	1.9843521098	1.9897809063
20	5.4981698322	5.4981455454	5.4981697199	1.9897809038	1.9843552066	1.9897809028
30	5.4981698290	5.4981456095	5.4981696708	1.9897809019	1.9843578113	1.9897808998
40	5.4981698203	5.4981456591	5.4981696247	1.9897808975	1.9843592922	1.9897808987

up to  $t = 40$ , solitary wave has *amplitude* = 0.52632. The values of the obtained conserved quantities  $I_M$ ,  $I_E$  and some other earlier results are given in Table 2. It can be observed from Table 2 that the percentage of relative changes of  $I_M$  and  $I_E$  are obtained as  $1.62 \times 10^{-8} \%$  and  $1.00 \times 10^{-10} \%$  for  $h = \Delta t = 0.1$ ;  $7.28 \times 10^{-8} \%$  and  $2.10 \times 10^{-8} \%$  for  $h = \Delta t = 0.05$ ;  $1.08 \times 10^{-7} \%$  and  $5.16 \times 10^{-8} \%$  for  $h = \Delta t = 0.025$ , respectively. Since the changes of the conserved quantities are less than  $1 \times 10^{-9}$ ,  $2 \times 10^{-10}$ , respectively, our scheme is sensibly conservative. The error norms  $L_2$  and  $L_\infty$  are satisfactorily small for different values of  $h$  and  $\Delta t$ . To make this observation, the error norms are determined and listed in Table 3. Also, Table 3 shows a comparison of the values of the obtained error norms with earlier results. We can say that our method provides good results than others. Figure 1(a) illustrates the motion of the single solitary wave profile from  $t = 0$  to  $t = 40$ . In addition, the motion of the solitary wave is depicted at specified times in Figure 1(b). It is clearly seen that the solitary wave moves to the right with a constant speed. Its amplitude and shape are preserved when time progresses, as expected. On the other hand, error graphs at time  $t = 40$  are plotted for different values of  $h$  and  $\Delta t$  in Figure 2.

### 6.2 Interaction of two solitary waves

Secondly, the interaction of two solitary waves is considered by using the initial condition given by the linear sum of two well separated solitary waves having different amplitudes

$$U(x, 0) = \sum_{i=1}^2 A_i \operatorname{sech}^4 [B_i (x - x_i)],$$

**Table 3.** Comparison of error norms for single solitary wave with  $a = b = c = 1, d = 0.5, v = 1.18$ , different values of  $h$  and  $\Delta t$ .

$h = \Delta t = 0.1$				$L_2 \times 10^3$			$L_\infty \times 10^3$		
$t$	<i>Present</i>	<i>CLDS</i> [7]	<i>SFEM</i> [2]	<i>Present</i>	<i>CLDS</i> [7]	<i>SFEM</i> [2]	<i>Present</i>	<i>CLDS</i> [7]	<i>SFEM</i> [2]
0	0.000000	0.000000	0.000000	0.000000	0.000000	0.000000	0.000000	0.000000	0.000000
10	0.370348	1.641934	0.356724	0.149073	0.631419	0.141639	0.253418	1.131442	0.244374
20	0.665684	3.045414	0.646705	0.336342	1.533771	0.326169	0.422656	1.878952	0.411492
30	0.924741	4.241827	0.902514						
40	1.187411	5.297873	1.162489						
$h = \Delta t = 0.05$				$L_2 \times 10^4$			$L_\infty \times 10^4$		
$t$	<i>Present</i>	<i>CLDS</i> [7]	<i>SFEM</i> [2]	<i>Present</i>	<i>CLDS</i> [7]	<i>SFEM</i> [2]	<i>Present</i>	<i>CLDS</i> [7]	<i>SFEM</i> [2]
0	0.000000	0.000000	0.000000	0.000000	0.000000	0.000000	0.000000	0.000000	0.000000
10	0.888927	4.113510	0.854386	0.362314	1.582641	0.343706	0.649564	2.835874	0.627075
20	1.823510	7.631169	1.779040	1.000742	3.843906	0.975412	1.320897	4.709118	1.293116
30	2.862236	10.62971	2.810186						
40	3.842086	13.27645	3.783328						
$h = \Delta t = 0.025$				$L_2 \times 10^4$			$L_\infty \times 10^5$		
$t$	<i>Present</i>	<i>CLDS</i> [7]	<i>SFEM</i> [2]	<i>Present</i>	<i>CLDS</i> [7]	<i>SFEM</i> [2]	<i>Present</i>	<i>CLDS</i> [7]	<i>SFEM</i> [2]
0	0.000000	0.000000	0.000000	0.000000	0.000000	0.000000	0.000000	0.000000	0.000000
10	0.357059	1.028173	0.351702	1.421479	3.965867	1.420544	0.925408	1.905450	0.916735
20	0.925408	1.905450	0.916735	3.264848	7.097948	3.258903	1.057023	2.650990	1.043479
30	1.057023	2.650990	1.043479	4.742297	9.610332	4.681364	1.183710	3.306738	1.183139
40	1.183710	3.306738	1.183139	4.846861	11.76011	4.847163			

where  $A_i = \frac{210bB^2}{13d^4}, B_i = \left| \sqrt{\frac{b}{52c v_i}} \right|, i = 1, 2, v_i$  and  $x_i$  are arbitrary constants. For the simulation, the parameters are taken to be  $a = b = c = 1, d = 0.5, h = 0.1, \Delta t = 0.1, v_1 = 0.3, v_2 = 0.5, x_1 = -70$  and  $x_2 = -35$  over the interval  $[-100, 400]$ . Computations are carried out up to  $t = 250$ . Numerical values of the conserved quantities  $I_M$  and  $I_E$  are computed. Obtained results are compared with earlier result in Table 4.

**Table 4.** Comparison of conserved quantities for the interaction of two solitary waves with  $a = b = c = 1, d = 0.5, h = \Delta t = 0.1, v_1 = 0.3, v_2 = 0.5, x_1 = -70$  and  $x_2 = -35$ .

$t$	$I_M$		$I_E$	
	<i>Present</i>	<i>SFEM</i> [2]	<i>Present</i>	<i>SFEM</i> [2]
0	19.3547763167	19.3547763167	23.4555195115	23.4555195111
50	18.6623337576	18.6976052814	23.4536464802	23.4623857679
100	18.5390343997	18.6524580290	23.7608289302	23.4627919923
150	18.4552610055	18.6849314916	23.2253266413	23.4648227878
200	18.5431101281	18.6798456059	23.6865522135	23.4658462283
250	18.8263024425	18.6670839625	23.7667431211	23.4662281908

It is seen that the obtained values of the conserved quantities remain constant sensibly during the computation. Figure 3(a) shows the interaction of two solitary waves profile from  $t = 0$  to  $t = 250$ . Also, the interaction of two solitary waves is illustrated at specified times in Figure 3(b).

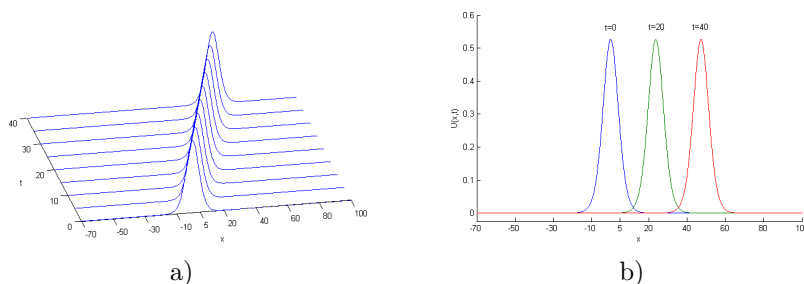


**Figure 1.** Results for  $a = b = c = 1, d = 0.5, v = 1.18$  and  $h = \Delta t = 0.1$ : a) single solitary wave profile, b) motion of single solitary wave at specified times.

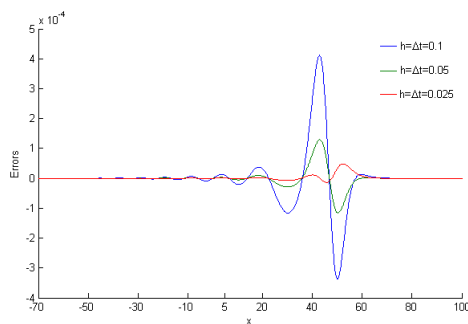


**Figure 2.** Errors for  $a = b = c = 1, d = 0.5, v = 1.18$ , different values of  $h$  and  $\Delta t$  at  $t = 40$ .

It is clear from the figure that, at  $t = 0$  the greater soliton at the left position of the smaller soliton, at the beginning of the run. With the increases of the time the greater soliton catches up the smaller until at time  $t = 80$ , then smaller soliton is absorbed. The overlapping process continues until  $t = 150$ , greater soliton has overtaken the smaller and get in the process of the separating. At time  $t = 250$ , the interaction is completed and the greater soliton has separated completely. At the end of this process, the solitary waves preserve their original shapes.

### 6.3 Interaction of three solitary waves

Thirdly, the behavior of the interaction of three solitary waves is studied for different amplitudes. So, the equation (1.1) is considered with initial condition given by the linear sum of three well-separated solitary waves of different amplitudes

$$U(x, 0) = \sum_{i=1}^3 A_i \operatorname{sech}^4 [B_i (x - x_i)],$$

where  $A_i = \frac{210bB_i^2}{13d}$ ,  $B_i = \left\lfloor \sqrt{\frac{b}{52cv_i}} \right\rfloor$ ,  $i = 1, 2, 3$ ,  $v_i$  and  $x_i$  are arbitrary constants. For the computational work, parameters  $a = b = c = 1, d = 0.5, h = 0.1$ ,

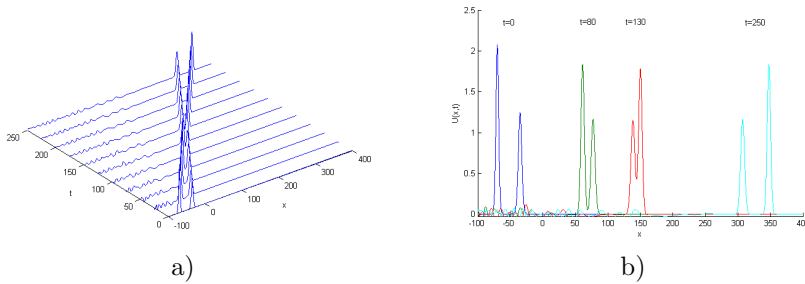


**Figure 3.** Two solitary waves for  $a = b = c = 1, d = 0.5, h = \Delta t = 0.1, v_1 = 0.3, v_2 = 0.5, x_1 = -70$  and  $x_2 = -35$ : a) profiles of waves, b) interaction of waves at specified times.

$\Delta t = 0.1, v_1 = 0.3, v_2 = 0.5, v_3 = 0.8, x_1 = -70, x_2 = -40$  and  $x_3 = -15$  are used over the interval  $[-100, 400]$ . Computations are done up to time  $t = 250$ . Table 5 displays a comparison of the values of the obtained conserved quantities with earlier result.

**Table 5.** Comparison of conserved quantities for the interaction of three solitary waves with  $a = b = c = 1, d = 0.5, h = \Delta t = 0.1, v_1 = 0.3, v_2 = 0.5, v_3 = 0.8, x_1 = -70, x_2 = -40$  and  $x_3 = -15$ .

$t$	$I_M$		$I_E$	
	<i>Present</i>	<i>SFEM</i> [2]	<i>Present</i>	<i>SFEM</i> [2]
0	26.0335670001	26.0335670001	27.0338255161	27.0338255158
50	25.3550323831	25.3912010200	27.0293369619	27.0410243545
100	25.0758817203	25.1890637167	27.3444359582	27.0421570504
150	25.0488953506	25.1729836835	27.7513876823	27.0438944266
200	25.0782292892	25.1975503011	27.0055964599	27.0448261554
250	25.3776582117	25.1823024487	27.7938004912	27.0452250712

It is clear from Table 5 that the obtained values for  $I_M$  and  $I_E$  are remain almost during the computer run. In Figure 4(a), the interaction of three solitary waves profile is depicted from  $t = 0$  to  $t = 250$ . Also, the interaction of three solitary waves is shown at specified times in Figure 4(b). As it is seen from the Figure 4, interaction started about time  $t = 50$ , overlapping processes occurred between time  $t = 50$  and  $t = 170$  and waves started to resume their original shapes after the time  $t = 250$ . At the end of this process, the solitary waves preserve their original shapes.

### 6.4 Evolution of solitons

In this section, we observe the evolution of solitons for the Rosenau-KdV equation (1.1) by using the undular bore initial condition. The evolution of a train of solitons for Rosenau-KdV equation is studied by using the undular bore initial condition

$$U(x, 0) = 0.5U_0 [1 - \tanh (|x - x_0|/d)]$$

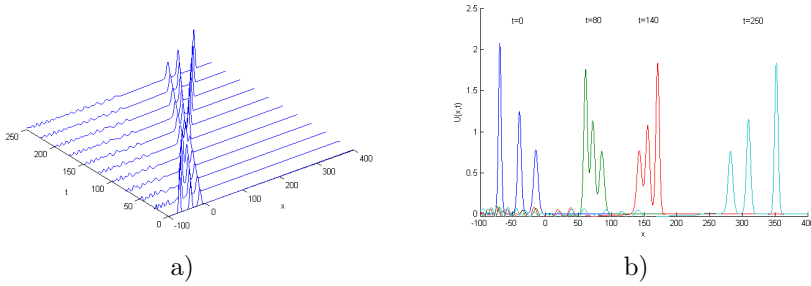


**Figure 4.** Three solitary waves for  $a = b = c = 1, d = 0.5, h = \Delta t = 0.1, v_1 = 0.3, v_2 = 0.5, v_3 = 0.8, x_1 = -70, x_2 = -40$  and  $x_3 = -15$ : a) profiles of waves, b) interaction of waves at specified times.

and boundary condition

$$U(-50, t) = U(350, t) = 0, \quad t > 0$$

to produce a train of solitons depending upon the value  $c$ .  $U(x, 0)$  denotes the elevation of the water above the equilibrium surface at time  $t = 0$ . The change in water level of magnitude  $U_0$  is centered on  $x = x_0$  and  $d$  measures the steepness of the change. The smaller the value of  $d$  the steeper is the slope. Parameters are taken as  $a = b = c = 1, d = 0.5, v = 1.18, h = 0.1, \Delta t = 0.1, U_0 = 1, x_0 = 25$  and  $d = 5$ . Calculations with these parameters are carried out up to the time  $t = 150$ . The computed two conserved quantities are compared with earlier result in Table 6.

**Table 6.** Comparison of conserved quantities for undular bore initial condition with  $a = b = c = 1, d = 0.5, v = 1.18$  and  $h = \Delta t = 0.1$ .

$t$	$I_M$		$I_E$	
	<i>Present</i>	<i>SFEM</i> [2]	<i>Present</i>	<i>SFEM</i> [2]
0.0	50.0000031022	50.0000031022	45.0046265340	45.0046240676
25	49.9949769132	49.9962032980	45.0046302283	45.0046392765
50	49.9912936179	49.9953438219	45.0047336077	45.0046467879
75	49.9825407041	49.9926519881	45.0059017563	45.0046494681
100	49.9728554453	49.9947407323	45.0104670928	45.0046572374
125	49.9513627796	49.9933952569	45.0284774099	45.0046645828
150	49.9183079349	49.9916251623	48.0853413051	45.0046688213

It is seen from the table that the values of the invariants are virtually preserved. Figure 5(a) shows that the evolution of solitons profiles with undular bore initial condition from  $t = 0$  to  $t = 150$ . Also, evolution of solitons is depicted at specified times in Figure 5(b). As it is seen from these figures, the initial perturbation evolves into a good developed train of solitons. As the time progresses, six solitons moving to the right are observed.

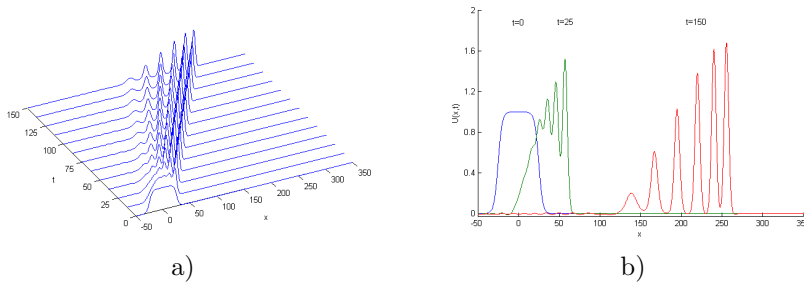


**Figure 5.** Developed train for  $a = b = c = 1$ ,  $d = 0.5$ ,  $v = 1.18$  and  $h = \Delta t = 0.1$  of: a) solitons profile, b) solitons at specified times.

## 7 Conclusions

In this paper, to study the dynamics of the dispersive shallow water waves, it is studied on Rosenau-KdV equation with various test problems. Numerical simulations for Rosenau-KdV equation are proposed using a collocation method with the septic B-spline interpolation functions. The accuracy of obtained schemes schemes is shown by calculating error norms  $L_2$  and  $L_\infty$ . The stability analysis of the method is shown to be unconditionally stable. The obtained schemes are tested through a single solitary wave in which the analytic solution is known, then extend it to study the interaction of solitary waves and evolution of solitons where no analytic solution is known. The obtained numerical results and simulations show that applied method is an efficient method to analyze behaviors of the dispersive shallow water waves.

## References

- [1] T. Ak, S.B.G. Karakoc and A. Biswas. Numerical simulation of dispersive shallow water waves with an efficient method. *Journal of Computational and Theoretical Nanoscience*, **12**(12):5995–6001, 2015. <https://doi.org/10.1166/jctn.2015.4748>.
- [2] T. Ak, S.B.G. Karakoc and H. Triki. Numerical simulation for treatment of dispersive shallow water waves with Rosenau-KdV equation. *The European Physical Journal Plus*, **131**(10):356–370, 2016. <https://doi.org/10.1140/epjp/i2016-16356-3>.
- [3] A. Biswas, H. Triki and M. Labidi. Bright and dark solitons of the Rosenau-Kawahara equation with power law nonlinearity. *Physics of Wave Phenomena*, **19**(1):24–29, 2011. <https://doi.org/10.3103/S1541308X11010067>.
- [4] P.B. Bochev and M.D. Gunzburger. *Least-squares finite element methods*. Springer, New York, 2009.
- [5] H. Demiray. Higher order approximations in reductive perturbation methods: strongly dispersive waves. *Communications in Nonlinear Science and Numerical Simulation*, **10**(5):549–558, 2005. <https://doi.org/10.1016/j.cnsns.2003.08.004>.
- [6] A. Esfahani. Solitary wave solutions for generalized Rosenau-KdV equation. *Communications in Theoretical Physics*, **55**(3):396–398, 2011. <https://doi.org/10.1088/0253-6102/55/3/04>.

- [7] J. Hu, Y. Xu and B. Hu. Conservative linear difference scheme for Rosenau-KdV equation. *Advances in Mathematical Physics*, **2013**:1–7, 2013. <https://doi.org/10.1155/2013/423718>.
- [8] S.B.G. Karakoc and T. Ak. Numerical simulation of dispersive shallow water waves with Rosenau-KdV equation. *International Journal of Advances in Applied Mathematics and Mechanics*, **3**(3):32–40, 2016.
- [9] S.B.G. Karakoc and T. Ak. Numerical solution of Rosenau-KdV equation using subdomain finite element method. *New Trends in Mathematical Sciences*, **4**(1):223–235, 2016. <https://doi.org/10.20852/ntmsci.2016115857>.
- [10] D.J. Korteweg and G. de Vries. XLI. on the change of form of long waves advancing in a rectangular canal, and on a new type of long stationary wave. *Philosophical Magazine Series 5*, **39**(240):422–443, 1895. <https://doi.org/10.1080/14786449508620739>.
- [11] P.M. Prenter. *Splines and variational methods*. John Wiley, New York, 1975.
- [12] P. Razborova, B. Ahmed and A. Biswas. Solitons, shock waves and conservation laws of Rosenau-KdV-RLW equation with power law nonlinearity. *Applied Mathematics & Information Sciences*, **8**(2):485–491, 2014. <https://doi.org/10.12785/amis/080205>.
- [13] P. Razborova, A.H. Kara and A. Biswas. Additional conservation laws for Rosenau-KdV-RLW equation with power law nonlinearity by Lie symmetry. *Nonlinear Dynamics*, **79**(1):743–748, 2015. <https://doi.org/10.1007/s11071-014-1700-y>.
- [14] P. Razborova, L. Moraru and A. Biswas. Perturbation of dispersive shallow water waves with Rosenau-KdV-RLW equation with power law nonlinearity. *Romanian Journal of Physics*, **59**(7-8):658–676, 2014.
- [15] P. Razborova, H. Triki and A. Biswas. Perturbation of dispersive shallow water waves. *Ocean Engineering*, **63**:1–7, 2013. <https://doi.org/10.1016/j.oceaneng.2013.01.014>.
- [16] P. Rosenau. A quasi-continuous description of a nonlinear transmission line. *Physica Scripta*, **34**(6B):827–829, 1986. <https://doi.org/10.1088/0031-8949/34/6b/020>.
- [17] P. Rosenau. Dynamics of dense discrete systems. *Progress of Theoretical Physics*, **79**(5):1028–1042, 1988. <https://doi.org/10.1143/PTP.79.1028>.
- [18] A. Saha. Topological 1-soliton solutions for the generalized Rosenau-KdV equation. *Fundamental Journal Mathematical Physics*, **2**(1):19–25, 2012.
- [19] P. Sanchez, G. Ebadi, A. Mojaver, M. Mirzazadeh, M. Eslami and A. Biswas. Solitons and other solutions to perturbed Rosenau-KdV-RLW equation with power law nonlinearity. *Acta Physica Polonica A*, **127**(6):1577–1586, 2015. <https://doi.org/10.12693/APhysPolA.127.1577>.
- [20] E. Süli and D.F. Mayers. *An introduction to numerical analysis*. Cambridge University Press, Cambridge, 2003. <https://doi.org/10.1017/CBO9780511801181>.
- [21] V. Thomee. *Galerkin finite element methods for parabolic problems*. Springer-Verlag, Berlin, 2006.
- [22] H. Triki, T. Ak, S.P. Moshokoa and A. Biswas. Soliton solutions to KdV equation with spatio-temporal dispersion. *Ocean Engineering*, **114**:192–203, 2016. <https://doi.org/10.1016/j.oceaneng.2016.01.022>.

- [23] B. Wongsaijai and K. Pochinapan. A three-level average implicit finite difference scheme to solve equation obtained by coupling the Rosenau-KdV equation and the Rosenau-RLW equation. *Applied Mathematics and Computation*, **245**:289–304, 2014. <https://doi.org/10.1016/j.amc.2014.07.075>.
- [24] M. Zheng and J. Zhou. An average linear difference scheme for the generalized Rosenau-KdV equation. *Journal of Applied Mathematics*, **2014**:1–9, 2014. <https://doi.org/10.1155/2014/202793>.
- [25] J.-M. Zuo. Solitons and periodic solutions for the Rosenau-KdV and Rosenau-Kawahara equations. *Applied Mathematics and Computation*, **215**(2):835–840, 2009. <https://doi.org/10.1016/j.amc.2009.06.011>.